

# INFLUENCE OF THERMOPHYSICAL PROPERTIES ON TRANSFER OF HEAT IN MULTI-LAYER DUCTS AND TEMPERATURE CONTROL USING ELECTRIC HEATING

W. O. Pedruzzi<sup>a</sup>,  
W. B. Silva<sup>b</sup>  
and J. C. S. Dutra<sup>c</sup>

<sup>a, b, c</sup> Universidade Federal do Espírito Santo  
Centro de Ciências Agrárias e Engenharias  
Departamento de Engenharia Rural  
Alto Universitário  
29500-000, Alegre, Espírito Santo, Brazil  
wancley.pedruzzi@edu.ufes.br<sup>a</sup>,  
wellington.betencurte@ufes.br<sup>b</sup>,  
julio.dutra@ufes.br<sup>c</sup>

Received: Feb 9, 2023

Reviewed: Feb 26, 2023

Accepted: Mar 01, 2023

## ABSTRACT

Ensuring oil production flow in offshore systems is a critical aspect of oil exploration operations. Any interruption in the production process, whether partial or complete, can result in significant financial losses and cause solid deposition in the production line. Such deposition is due to the crystallization of paraffin and hydrates, a common problem caused by low temperatures in deep waters. Among various mitigation strategies, the Pipe-in-Pipe (PIP) system with active heating is a technological solution to address this issue. This work aimed to perform a numerical simulation of the PIP system using the Finite Volume Method with an implicit formulation, considering the effect of temperature on fluid properties and the system's dynamic response. A control loop using a PI velocity algorithm was developed to maintain the temperature above the critical point. Such simulation studies were performed using the Python programming language in the Anaconda suite. The results showed that the fluid properties greatly influence the dynamic response. The PI control maintained the temperature in the desired condition, demonstrating its operational effectiveness in preventing solid deposition and delivering stable and low-oscillatory behavior. This research emphasizes the significance of taking temperature's impact on fluid properties into account when simulating offshore oil production systems and demonstrates the effectiveness of implementing feedback control.

**Keywords:** pipe-in-pipe system; finite volume method; process control

## NOMENCLATURE

$c_p$	specific heat, J/(kg.°C)
$C$	dimensionless specific heat
$g$	prescribed heat flux, W/m <sup>3</sup>
$G$	dimensionless heat flow
$h$	thermal exchange coefficient, W/(m <sup>2</sup> °C)
$k$	thermal conductivity, W/(m°C)
$K$	dimensionless thermal conductivity
$P$	dimensionless specific mass
$t$	time, h
$T$	temperature, °C

## Greek symbols

$\theta$	dimensionless temperature
$\rho$	specific mass, kg/m <sup>3</sup>
$\tau$	dimensionless time

## Subscripts

0	initial
i	pip layer
$\infty$	ocean

## INTRODUCTION

Production in offshore fields, mainly in deep and ultra-deep waters, presents characteristic challenges for flow assurance. The deposition of paraffin and hydrates along the production pipelines is critical. It occurs due to the working condition in deep waters: the consequent temperature profiles (MATOS, 2019). In conditions of production shutdowns and closure of safety valves, blocking the fluid flow, the low temperature of seawater accentuates the formation of solid particles (VIANNA, 2010).

Pipe-in-pipe (PIP) systems, or multi-layer piping, are widely used in the modern oil industry in deep water conditions; this is due to their effect of efficient thermal insulation (BI; HAO, 2016). A conventional PIP system comprises an outer tube, an inner tube, and a layer of insulation filling the region between them. This type of physical structuring is characteristic of a compliant PIP system (KARAMPOUR et al., 2017 apud GUO et al., 2020).

Integrating this system with active heating, regarding the problem of deposition in PIP pipelines, is essential for the flow guarantee project in deep water pipelines. This strategy improves thermal insulation

and prevents the oil temperature from reaching a critical condition of solid deposition (AN; SU, 2015).

With the increasing distance between the wells and the processing unit, temperature monitoring solutions associated with control strategies have become essential to understand the process condition and establishing operational policies. Therefore, this work investigated the numerical simulation and heating control of a PIP system, using the Finite Volume method with implicit formulation with a Proportional-Integral (PI) controller adjusted through the Internal Model Control technique (IMC). The simulations considered a production shutdown, where the fluid inside the pipelines is stagnant.

### Physical Problem Formulation

The physical problem under analysis was proposed by VIANNA (2010), based on a duct system composed of two concentric tubes equipped with direct electric heating and insulating material between the internal and external duct (Figure 1).

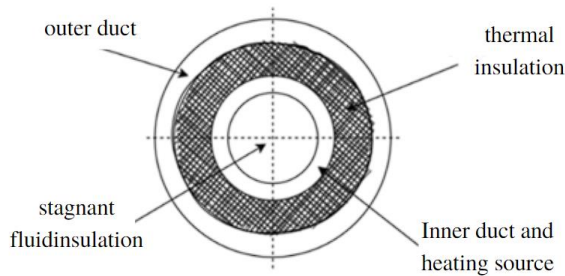


Figure 1. Complete model formed by multiple layers.  
Source: VIANNA (2010), adapted by the authors.

### Mathematical Model

The model comprises the phenomenon of heat conduction through the pipe walls and in the stagnant fluid and the convection on the outer surface of the wall in contact with the ocean. The two concentric ducts of the PIP system give rise to four cylindrical layers, considered homogeneous, isotropic, and those adjacent to have perfect thermal contact. All thermophysical properties are constant except in the stagnant fluid layer (VIANNA, 2010). Thus, the mathematical formulation in cylindrical coordinates is given by the partial differential equation:

$$\rho_i C_{p_i} \frac{\partial T_i(r, t)}{\partial t} = \frac{1}{r} \frac{\partial}{\partial r} \left( r k_i \frac{\partial T_i(r, t)}{\partial r} \right) + g_i(r, t) \quad \text{in } r_i \leq r \leq r_{i+1}; t > 0 \quad (6)$$

Where  $i$  represents each layer of the PIP, being 0 to 3 for the stagnant fluid layer, the inner duct layer, the heat-insulating layer, and the outer duct layer.

The boundary conditions are:

1. Neumann-type symmetry condition.

$$-k_0(T) \frac{\partial T_0(r, t)}{\partial r} = 0; \text{ in } r = 0; t > 0 \quad (2)$$

2. Neumann-type perfect thermal contact condition.

$$\left. \begin{aligned} T_i &= T_{i+1} \\ k_i(T) \frac{\partial T_i(r, t)}{\partial r} &= k_{i+1}(T) \frac{\partial T_{i+1}(r, t)}{\partial r} \end{aligned} \right\};$$

$$\text{in the interfaces } r = r_{i+1}, i = 0, \dots, 2, t > 0 \quad (3)$$

3. Robin-type convection heat exchange condition.

$$\left. \begin{aligned} k_3 \frac{\partial T_3(r, t)}{\partial r} + h T_3(r, t) &= h T_\infty; \\ \text{in } r = r_4, t > 0 \end{aligned} \right\} \quad (4)$$

4. Initial condition.

$$T_i(r, 0) = T_{i_0}, \text{ in } t = 0, \forall r \quad (5)$$

According to VIANNA (2010), this model can be scaled to reduce the variables involved in the model and the distance between the points of the time mesh. The dimensionless groups are:

$$\theta(R, \tau) = \frac{T_i(r, t) - T_\infty}{T_0 - T_\infty}; \tau = \frac{k^* t}{\rho^* C_p^* r^{*2}}; R = \frac{r}{r^*} \quad (6)$$

$$P_i = \frac{\rho_i}{\rho^*}; C_i = \frac{C_{p_i}}{C^*}; K_i = \frac{k_i}{k^*} \quad (7)$$

$$G = \frac{r^{*2} g}{k T^*}; Bi = \frac{h r^*}{k} \quad (8)$$

Thus, an equation is formed for each PIP domain and its boundary conditions. This set of equations was solved using the Finite Volume method, with an implicit formulation in which the properties of the fluid vary with temperature.

### Finite Volume Method

According to Maliska (1995), there are two ways to obtain the approximate equations in the finite volume method. The first is based on performing the balance of the property in question in the volumes. The second is integrating the differential equation's conservative form in its elementary control volume in space and time. The representation of the elementary control volume can be seen in Figure 2.

The temporal discretization of the equations can be explicit, partially implicit, or fully implicit (MALISKA, 1995). The fully implicit formulation used here evaluates all the temperatures surrounding the point P at the same instant, leading to the formation of a coupled equation system. This formulation is used more frequently since it confers numerical stability.

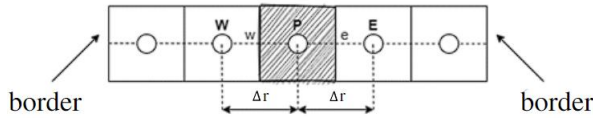


Figure 2. Representation of the elementary volume.  
Source: VIANNA (2010), adapted by the authors.

However, in the stagnant fluid domain, there is the problem that the properties vary with temperature. Integration with the implicit method would be highly complex and computationally costly if each property were estimated at the current time. Vianna (2010) calculated each property at the nodal point of the control volume based on the previous temperature value. This same consideration was made in this work.

Thermal conductivity, in particular, is evaluated at the interfaces. As the implicit algorithm always marches between the nodal points of each volume, this property can be calculated from a harmonic mean between adjacent points (PATANKAR, 1980), with the average value at each interface given by:

$$K_{0w}(\theta) = \frac{2K_{0W}K_{0P}}{K_{0W} + K_{0P}} \quad (9)$$

$$K_{0e}(\theta) = \frac{2K_{0E}K_{0P}}{K_{0E} + K_{0P}} \quad (10)$$

These equations were used to calculate the conductivity at the fluid domain interfaces and for all interfaces present in the PIP system. According to Vianna (2010), the thermophysical properties of the stagnant fluid are expressed by a linear variation with temperature as follows:

$$\begin{aligned} \rho(T) &= A_1T + A_2; \quad C_p(T) = B_1T + B_2; \\ k(T) &= C_1T + C_2 \end{aligned} \quad (11)$$

Where the thermophysical properties and parameters are given in Tables 1 and 2, the units are per the international system.

## RESULTS AND DISCUSSION

The verification of the proposed solution was performed based on the comparison of the results obtained by Vianna (2010), who implemented the model using the explicit formulation, and the results obtained by Araujo et al. (2017), who used the implicit formulation using constant properties of the fluid.

As a case study, the stagnant fluid was adopted with an initial temperature of 80 °C, a seawater temperature of 4 °C, and an external heat transfer coefficient of 2035 [W/m<sup>2</sup>°C]. The critical temperature at which deposit formation occurs was considered 20 C, and the properties of the medium and the constant parameters are contained in Table 1. The discretization of the space was the same as Vianna

(2010), in which the domain is composed of 50 volumes, 30 for the fluid layer, 5 for the inner duct layer, 10 for the thermal insulation layer, and 5 for the outer duct. Since it is an implicit formulation, the discretization of time is not limited by the stability criterion, though it can change the convergence of the result (MALISKA, 1995). In this work, 500 partitions were initially adopted for the time domain.

Table 1. Thermophysical parameters and properties.

Propertie s	Inner duct	Thermal insulation	Outer duct	Sea water
Thermal conductivity	52.34	0.17	52.34	0.59
Specific mass	7700.00	750.00	7700.00	922.52
Specific heat	502.10	2000.00	502.10	3993.00
Internal diameter	0.20	-	0.35	-
External diameter	0.25	-	0.40	-
Composit ion	Carb. steel	Polypropyl ene	Carb. steel	Water

Table 2. Parameters of the thermophysical properties of the fluid.

Parameter	Value
A <sub>1</sub>	-0.5535
A <sub>2</sub>	966.7991
B <sub>1</sub>	5.1186
B <sub>2</sub>	1519.7178
C <sub>1</sub>	-0.0001
C <sub>2</sub>	0.1304

The simulation was performed using Python language in the Anaconda packet. The machine's processor is AMD Ryzen 5 3400G, with 3.70 GHz and available RAM of 16 GB.

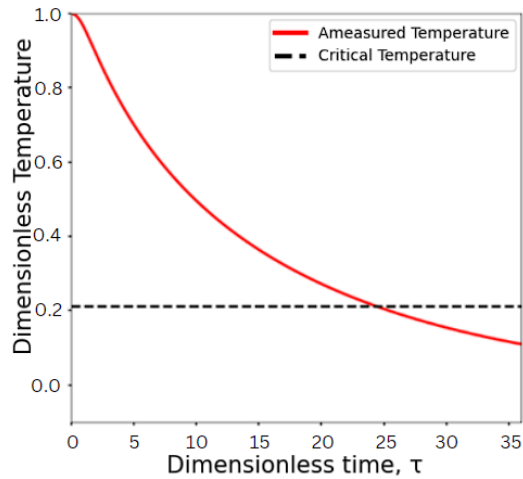
First, a qualitative analysis was performed via a visual comparison of the result obtained in this work with those from Vianna (2010), as shown in Figure 3.

It is possible to observe that Vianna (2010) obtained an uncertain solution profile, a region encompassing the measurements with a standard deviation of 2 °C. Such an approach resulted in a temperature field, as its purpose was to simulate an uncertainty associated with the measurement. The solution obtained in this work is contained within this region of calculated measurements.

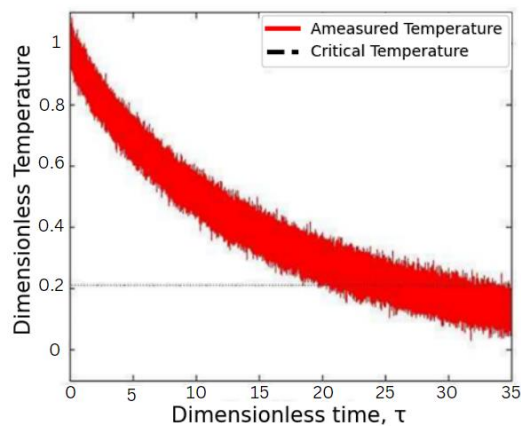
It can be seen that the dimensionless time required for the temperature to reach the critical temperature in solution (3a) was approximately equal to 25. In contrast, solution (3b) shows that this instant is between 20 and 35 dimensionless times.

Based on the results presented by Araujo et al. (2017), the influence of the variant fluid properties can be verified, as shown in Figure 4. The difference is

noticeable when the effect resulting from the variation of fluid properties over time is neglected. Such authors obtained approximately 35 units of dimensionless time for the temperature to reach the crystallization condition, using 33 volumes for the insulating layer. In this work, as seen in (3a), it was possible to obtain a result close to that of Vianna (2010) with the same simulation configuration.



(3a)



(3b)

Figure 3. Comparison of the temperature profile over time at the measurement point, located on the surface of the inner duct: (3a) solution of this work; (3b) solution by Vianna (2010).

The average temperatures for dimensionless times from 0 to 40.614 were analyzed and compared to the modification in the number of elementary volumes. Also, the time for the temperature to reach the critical condition was computed. The results are provided in Table 3.

Note that the number of elementary volumes and the time for the inner duct surface to reach the critical temperature are proportional. One explanation is the increase in elementary volumes in the insulating layer. When the number of volumes in this domain increases,

this layer's influence to mitigate the thermal exchange effects becomes evident. Consequently, the average temperature at the measurement point increases as less heat is lost to the external environment (seawater).

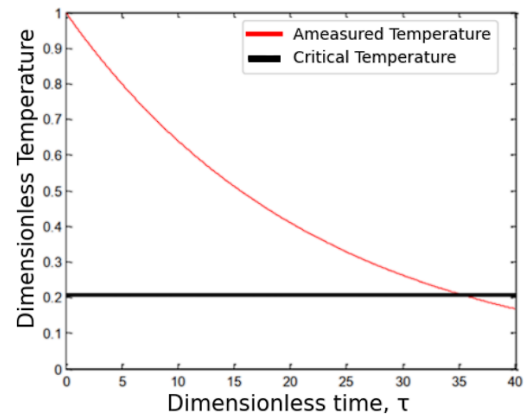


Figure 4. Temperature profile at the measurement point, located on the surface of the inner duct: solution by Araujo et al. (2017).

Table 3. Convergence test results.

Number of Elementary Volumes	Temporal mesh	Average temperature at the measurement point	Dimensionless time to reach critical temperature [-]
50	500	0.3494	24.6500
250	500	0.3601	24.9215
500	500	0.3615	24.9898
1500	500	0.3624	25.0349
2000	500	0.3625	25.0405
3000	500	0.3626	25.0462
50	3000	0.3485	24.312
50	10000	0.3483	24.3035
50	30000	0.3483	24.3034

As for the variation in the number of discrete points for time, an inverse response occurs: the smaller the time difference between the points, the fluid will cool down moderately faster until it reaches the critical temperature. This phenomenon is linked to the varying properties of the fluid. In Figure 4, it was possible to observe that neglecting its effects results in a dimensionless time until the phenomenon of crystallization occurs, more significant than that stipulated by Vianna (2010). So, when refining the mesh, the effects of property variations over time intensify.

Given the convergence analysis presented in Table 3, it is possible to choose the configuration that provides good performance and computational speed, with that using 500 control volumes and 500 instants of time,

there is little difference in the temperature averages and low computational time.

As the fluid temperature tends to stay below the critical temperature as time passes, it is essential to develop a heating proposal to avoid this problem. Two heating scenarios are evaluated: first, a constant heating; and, subsequently, a PI-type feedback control to maintain the fluid temperature above 30 °C, using the described model to generate the measurements. The pairing between the controlled variable and the manipulated variable is, respectively, temperature ( $T$ ) and heat flux ( $g > 0$ ).

The tuning of the PI controller parameters was based on the internal model technique (IMC) (SEBORG *et al.*, 2011). An approximate linear model was generated according to the method by Sundaresan and Krishnaswamy (REDDY, 2019), simulating a collection of real data from synthetic measures obtained in front of a step in the manipulated variable ( $g$ ). The values of the tuned  $K_c$  and  $\tau_I$  parameters are, respectively, 35 and 80. The closed-loop simulation results can be seen in Figures 5 and 6.

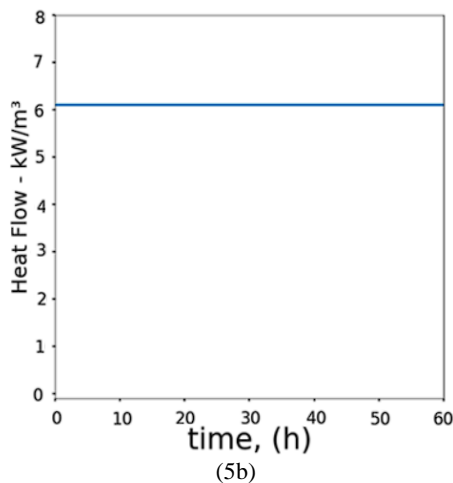
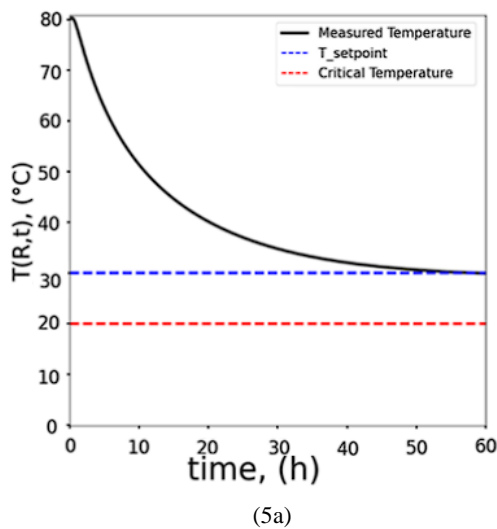


Figure 5. Constant electric heating. (5a) temperature response; (5b) fixed heat flux.

In Figure 5, it is observed that, with intermittent heating, adopting a constant heat flow of 6.1 kW/m<sup>3</sup>, it is possible to maintain the fluid temperature at the setpoint (nominal condition) of 30°C after 60 hours of heating. In Figure 6, the performance of the PI controller to maintain the temperature at the same setpoint is observed. Note that the control fulfills this objective, in which, in approximately 18 hours, the temperature is in the desired condition. The controller is activated after 15 hours of fluid stagnation to prevent the heat flux from being negative, representing cooling and not heating, which is undesirable and makes no physical sense. Furthermore, to evaluate the robustness of the controller, two servo tests were applied with a step of +5 °C at 27 hours and another step of -7 °C at 35 hours. The control was maintained with fast and stable responses.

Another analysis can be done by looking at the area under the curves generated for the heat flux. In constant heating, the region under the curve is much larger than that obtained with the controller, which results in a more significant expenditure of energy to heat the fluid. Thus, the control proposal becomes interesting because it provides lower energy costs.

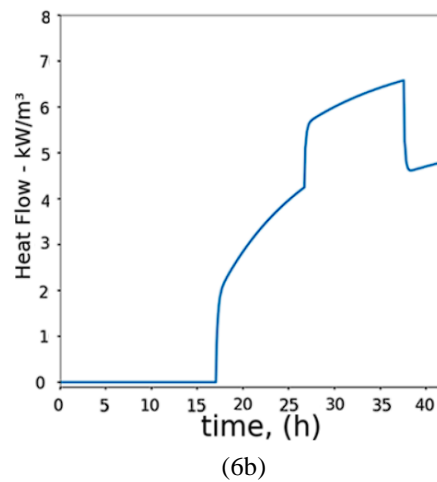
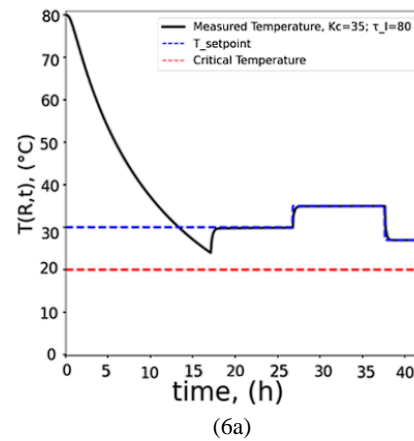


Figure 6. PI performance to control the temperature. (6a) temperature response; (6b) heat flux manipulation.

Finally, the closed-loop response was evaluated with the controller in front of measuring equipment with a standard deviation for the associated uncertainty of 2° C. The response can be seen in Figure 7. The controller performed satisfactorily, maintaining the temperature at the specified setpoint even with a poor-quality sensor.

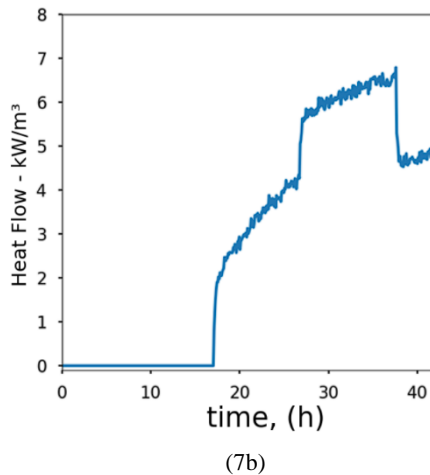
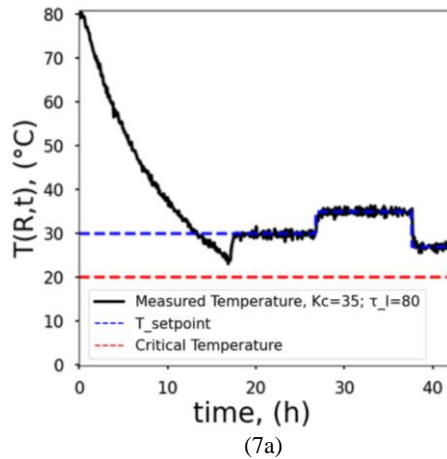


Figure 7. Performance of the PI controller against a noisy measurement with a standard deviation of 2 °C. (7a) temperature profile; (7b) heat flux profile.

## CONCLUSIONS

In this work, the temperature field of the pipe-in-pipe system was simulated using the Finite Volume method with implicit formulation, considering the thermophysical properties of the fluid varying with temperature and time.

The obtained results were satisfactory, considering its stability according to the convergence test. It is worth noting that the method employed is not associated with the stability criterion of the explicit solution adopted by Vianna (2010), resulting in a gain in computational time, which may modify the steps in time and space.

The control proposal for electric heating proved effective in keeping the temperature above the critical temperature and at the desirable temperature (setpoint), thus mitigating the possibility of deposits appearing and allowing lower energy costs.

## ACKNOWLEDGEMENTS

To the National Council for Scientific and Technological Development - CNPq, for funding the research, through the Institutional Program of Scientific Initiation Scholarships of the Federal University of Espírito Santo.

## REFERENCES

- An, C.; Su, J. (2015), *Lumped models for transiente thermal analysis of multilayered composite pipeline with active heating*. Núcleo Interdisciplinar de Dinâmicas dos Fluido, Elsevier, in: Applied Thermal Engineering, v. 87. Doi: 10.1016/j.applthermaleng.2015.05.061.
- Araujo, M. N.; Mattos, L. C. N.; Fortunato, T. B.; Dutra, J. C. S.; Silva, W. B. (2017), Monitoramento da temperatura de óleo em um sistema de tubulação multicamadas utilizando filtro bayesiano asir. *Engevista*, v. 19, n. 3, p. 792-805. Doi: 10.22409/engevista.v19i3.910.
- Bai, Q.; Bai, Y. (2014), *Subsea pipeline design, analysis, and installation*. Oxford: Gulf Professional Publishing.
- Guo, Y; Zhu, B.; Zhao, X.; Chen, B.; Li, y. (2020), Dynamic characteristics and stability of pipe-in-pipe system conveying two-phase flow in thermal environment. *Applied Ocean Research*, v. 103. Doi: 10.1016/j.apor.2020.102333.
- Karampour, H; Alrsai, M.; Albermani, F.; Guan, H. (2017), Propagation Buckling in Subsea Pipe-in-Pipe Systems. *Journal of Engineering Mechanics*, v. 143.
- Maliska, C. R. (1995), *Transferência de Calor e Mecânica dos Fluidos Computacional. Laboratório de Simulação Numérica em Mecânica dos Fluidos e Transferência de Calor – SINMEC*.
- Matos, S. F.; Altoé, L. (2019), Análise da garantia de escoamento de petróleo em águas profundas em relação à deposição de parafina. *Latin American Journal of Energy Research – Lajer*, v. 6, n. 2, p. 12-31. Doi: 10.21712/lajer.2019.v6.n2.p12-31.
- Patankar, S. V. (1980), Numerical Heat Transfer and Fluid Flow. *Series in Computational Methods in Mechanics and Thermal Sciences*.
- Reddy, S. N.; Chidambaram, M. (2019), Model identification of critically damped second order plus time delay systems, *Indican Chemical Engineer*, v. 62. Doi: 10.1080/00194506.2019.1629842.
- Seborg, D. E.; Edgar, T. F.; Mellichamp, D. A.; Doyle III, F. J. (2011), *Process dynamics and control*. 3. ed. Nova Jersey: John Wiley & Sons.

Silva, W. B. (2008), *Otimização de Sistemas Ativos de Isolamento Térmico Multicamadas*. Dissertação de Mestrado, IME, Rio de Janeiro – RJ.

Vianna, F. L. V. (2010), *Estimação e Controle Ótimo Aplicado a Sistema de Aquecimento Ativo em Duto Multicamadas*. Tese de Doutorado, COPPE, Universidade Federal do Rio de Janeiro – RJ.